

1 Attenuation of high water levels over restored saltmarshes can be limited.

2 Insights from Freiston Shore, Lincolnshire, UK

3 Joshua Kiesel^{*a,c}, Mark Schuerch^{b,c}, Iris Möller^c, Tom Spencer^c, Athanasios Vafeidis^a

4
5 ^a Department of Geography, Christian Albrechts Universität zu Kiel, 24118, Germany

6 ^b Lincoln Center for Water and Planetary Health, School of Geography, University of
7 Lincoln, Brayford Pool Campus, Lincoln, LN6 7TS

8 ^c Cambridge Coastal Research Unit, Department of Geography, University of
9 Cambridge, CB2 3EN, UK

10 *Corresponding author

11 E-mail addresses: kiesel@geographie.uni-kiel.de (J. Kiesel), MSchuerch@lincoln.ac.uk

12 (M. Schuerch), im10003@cam.ac.uk (I. Möller), ts111@cam.ac.uk (T. Spencer),

13 vafeidis@geographie.uni-kiel.de (A. Vafeidis)

14 Declarations of interest: none

15 Abstract

16 The managed realignment (MR) of flood protection on low-lying coasts, and the
17 creation, or re-creation, of intertidal saltmarsh habitat between old and new, more
18 landward sea defence lines is an intervention designed to help protect coastal
19 infrastructure and communities against the impact of storm waves and surges.
20 However, the effectiveness of such schemes has rarely been proven in the field.
21 Environmental monitoring has generally been limited to the first few years after
22 implementation and has focussed on sediment accretion and surface elevation change,
23 vegetation establishment and habitat utilization, to the neglect of the study of
24 biophysical processes, such as wave energy dissipation and High Water Level (HWL)
25 attenuation. We address this knowledge gap by analysing HWL attenuation rates in

Abbreviations

HWL

high water level

MR

managed realignment

- 26 saltmarshes from within, and in front of, the open coast MR site of Freiston Shore
- 27 (Lincolnshire, UK).

Abbreviations
HWL
MR

high water level
managed realignment

28 For this purpose, a suite of 16 pressure transducers was deployed along four sections
29 (two within and two outside the MR) of identical setup to measure water level
30 variations during the highest spring tides of the year 2017.

31 Our results show that for the conditions encountered during the field monitoring
32 period, the capacity of the Freiston Shore MR site to provide HWL attenuation was
33 limited. HWL attenuation rates were significantly higher over the natural saltmarsh (in
34 front of the MR), where HWL attenuation ranged between 0 and 101 cm km^{-1} (mean
35 46 cm km^{-1}). Within the MR site, rates varied between -102 and 160 cm km^{-1} (mean -3
36 cm km^{-1}), with even negative attenuation (i.e. amplification) for about half of the
37 measured tides.

38 We argue that the weak performance of the MR site in terms of HWL attenuation was
39 a result of internal hydrodynamics caused by scheme design and meteorological
40 conditions. The latter may have counteracted the HWL attenuating effect caused by
41 the additional shallow water area provided by the restored saltmarsh.

42 *Keywords: coastal wetland, water level attenuation, restoration, managed*
43 *realignment, de-embankment, coastal protection*

44

451. Introduction

46 Acceleration of global sea level rise (Church et al., 2013; Nerem et al., 2018), land
47 subsidence (Syvitski et al., 2009) and an expected increase in the intensity of storms
48 and storm surges (Knutson et al., 2010) are threatening growing coastal populations

49 worldwide. Engineered coastal protection measures, such as dikes, seawalls or
50 embankments are costly to construct, maintain, and upgrade in order to keep pace
51 with sea level rise and increasing flood risk. Furthermore, embankments aggravate
52 land subsidence by promoting soil compaction due to drainage, and at the same time
53 impede sedimentation. In estuarine settings, embankments cause the funnelling of
54 flow, which ultimately leads to higher water levels up-estuary than would be the case
55 in more natural systems (Syvitski et al., 2009; Temmerman et al., 2013).

56 Nature-based coastal adaptation approaches are increasingly seen as a cost-effective
57 and sustainable flood and erosion protection option (Thorslund et al., 2017). Managed
58 realignment (MR) constitutes one approach towards nature-based coastal adaptation
59 and often involves the breaching or removal of hard coastal defences such as seawalls
60 and dikes and, at the same time, the construction of a new defence line further inland
61 (Esteves, 2013; Garbutt et al., 2006; Mazik et al., 2010). This allows for regular tidal
62 inundation of the realigned area, enabling the (re-)establishment of saltmarshes.
63 Furthermore, once established, saltmarshes should be self-sustaining, providing they
64 have sufficient accommodation space and sediment supply to keep pace with rates of
65 sea level rise (Kirwan et al., 2016; Schuerch et al., 2018).

66 MR aims at: 1) managing the risks associated with coastal hazards; and 2) creating, or
67 re-creating, habitats of high biodiversity and ecological value. Target 1) can be
68 subdivided into three elements. The first two elements have been referred to as along-
69 estuary attenuation (Smolders et al., 2015) and involve i) the creation of additional
70 flood storage and ii) the creation or re-establishment of additional wetland area

71 providing wider and 'rougher' estuarine boundaries to slow the passage of the flood
72 wave (Pethick, 2002; Townend and Pethick, 2002). The third aspect is represented by
73 iii) the reduction of water levels over the wetland itself, such that at the back of the
74 MR the new seawall can be of a lower design specification and cheaper to build and
75 maintain than the breached outer wall (Dixon et al., 1998; Pethick, 2002). This has
76 been referred to as within-wetland attenuation (Smolders et al., 2015) and constitutes
77 the focus of this paper. This form of attenuation is based on the simple physical
78 relationship between the drag forces exerted by rough surfaces, such as vegetated
79 wetlands, and resulting water surface slopes (i.e. the landward decrease in HWLs)
80 (Resio and Westerink, 2008) and attenuation of waves (Knutson et al., 1982; Möller et
81 al., 1999; Möller et al., 2014; Shepard et al., 2011).

82 There is good evidence that the presence of saltmarshes reduces surge and tidal levels
83 (Stark et al., 2015; Stark et al., 2016; Temmerman et al., 2012) over distances of 100s
84 of metres (Leonardi et al., 2018; Resio and Westerink, 2008). However, as of 2013, 66
85 % of MR schemes in England are smaller than 20 ha (Esteves, 2013), with only a few
86 schemes reaching several hundreds of metres in width. Thus, the dimensions of most
87 sites have the potential for effective wave reduction but the capacity for HWL
88 reduction remains unclear. Furthermore, it is well known that vegetation community
89 properties (Rupprecht et al., 2017; Tempest et al., 2015) and morphological surface
90 complexity (Loder et al., 2009; Temmerman et al., 2012) affect HWL attenuation.
91 These marsh characteristics are less well developed in MR sites compared to natural
92 systems (Lawrence et al., 2018; Mossman et al., 2012). Consequently, there is room for
93 debate as to whether or not the performance of restored saltmarshes (within MR

94 schemes), in terms of HWL reduction, is as effective as that recorded from natural
95 saltmarshes (Bouma et al., 2014). Answering this question involves the generation of
96 knowledge on both i) the maximum attenuation potential of coastal wetlands and ii)
97 the inundation thresholds up to which they are able to induce significant differences in
98 water surface slopes.

99 The Committee on Climate Change in the UK have argued that the length of realigned
100 shorelines in England needs to reach 550 km by 2030 (Committee on Climate Change,
101 2013). However, up until November 2013, only 66 km of England's shorelines had been
102 realigned, suggesting that considerable challenges lie ahead in order to reach the 2030
103 target. Whilst some of the resistance to MR implementation can be explained by
104 societal and political barriers to adoption (Cooper and McKenna, 2008), slow uptake
105 also suggests that the coastal defence case for MR has yet to be made in a sufficiently
106 convincing manner to significantly change operational coastal management practices.

107 One of the largest MR schemes in the UK was established in 2002 at Freiston Shore,

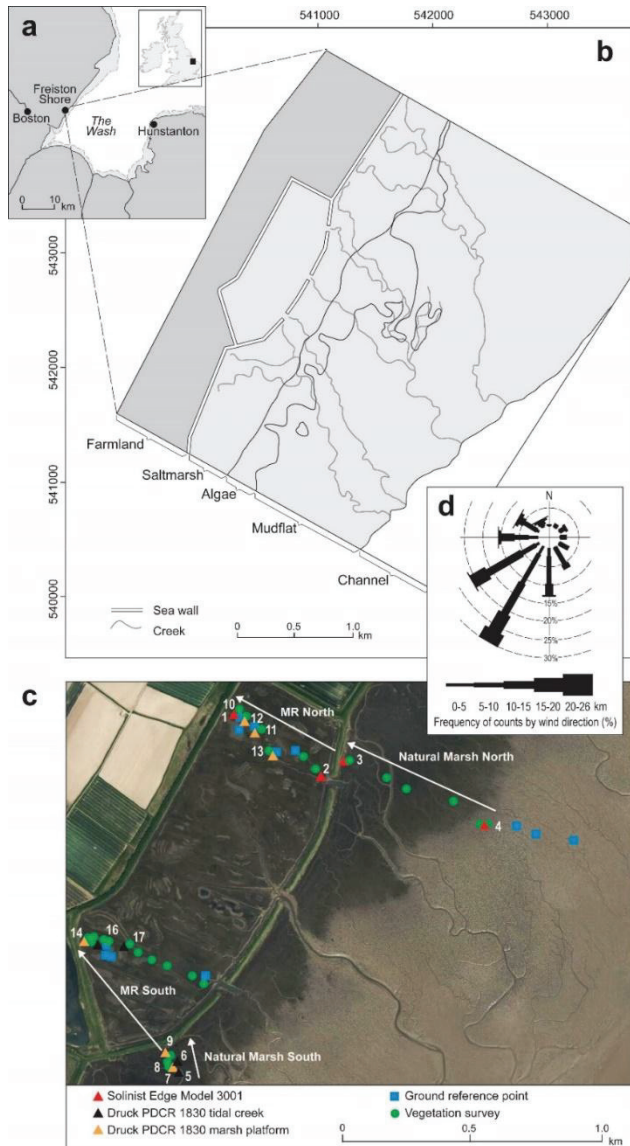


Figure 1: a) Location of the Freiston Shore managed realignment site in The Wash embayment, eastern England; b) schematic map of the managed realignment scheme including the adjacent natural saltmarsh and major tidal creeks; c) study design with location of pressure transducers and quadrats of the vegetation survey. White arrows indicate the four different sections along which the sensors were deployed; d) wind rose showing wind conditions for Holbeach weather station during the measurement period. (1.5-column)

108 Lincolnshire, UK (Figure 1). The targeted benefits of the site were specified as: 1) the
109 creation of more natural shorelines; 2) the reduction of flood protection costs; and 3)
110 habitat creation (Associated British Ports Marine Environmental Research (ABPmer),
111 2010). The UK Government's Department for Environment, Food & Rural Affairs
112 (DEFRA), its executive agency, the Environment Agency (EA) and the Natural
113 Environment Research Council (NERC) organized a monitoring campaign between 2002

114 and 2006, led by the Centre for Ecology and Hydrology, NERC, with additional
115 environmental monitoring and analysis by the Cambridge Coastal Research Unit
116 (University of Cambridge) and Birkbeck, University of London. The monitoring
117 programme focused on mapping from airborne platforms (aerial photography, light
118 detection and ranging (LiDAR) and compact airborne spectrographic imager (CASI)
119 surveys), establishing rates and patterns of sedimentation and accretion, and the
120 recording of vegetation communities, intertidal invertebrates, fish and bird population
121 dynamics and their change over time with the re-establishment of tidal exchange
122 (Brown et al., 2007). However those parameters initially targeted, i.e. the reduction of
123 flood protection costs, were not monitored after scheme implementation. The
124 incomplete evaluation of MR has often been ascribed to rather vague formulated
125 targets (Esteves, 2013; Esteves and Thomas, 2014; Wolters et al., 2005). This was also
126 the case at Freiston Shore. Not surprisingly, therefore, the formulation of clearly stated
127 objectives for future MR schemes was a recommendation in the final report (Brown et
128 al., 2007).

129 Addressing this coastal management knowledge gap is important, particularly when
130 considering the expected future need for considerably more MR schemes (Committee
131 on Climate Change, 2013). In this paper, we therefore address the following three
132 questions:

133 1. Has managed realignment at Freiston Shore led to a reduction in HWLs at the
134 landward margin of the realigned site?

135 2. How variable is HWL attenuation across space and over time within this MR
136 site?

137 3. For a specific range of tidal inundations, can a demonstrable difference be seen
138 in HWL attenuation between the MR scheme and the adjacent natural saltmarsh?

139

1402. **Study Area and Methods**

141 *2.1 Study area*

142 Freiston Shore was the largest MR in the UK at time of establishment in 2002 and still
143 ranks among the ten largest UK schemes (Associated British Ports Marine
144 Environmental Research (ABPmer), 2010). It is situated in The Wash embayment in
145 Lincolnshire (UK), southern North Sea (Figure 1a, 1b). 75 % of The Wash's coastline is
146 fronted by saltmarshes, which locally reach 1 – 2 km in width. The total saltmarsh area,
147 4,199 ha, constitutes the largest coherent area of active saltmarsh in the British Isles
148 (Pye, 1995). The tides of The Wash are characterized by a semidiurnal, macro-tidal
149 regime (mean spring tidal range (MSTR) = 6.5 m), exhibiting flood dominated tidal
150 asymmetry (Friess et al., 2014; Pye, 1995). Wave rider buoy measurements at the
151 mouth of The Wash, between May 1999 and May 2000, recorded maximum and mean
152 significant wave heights of 2.81 and 0.61 m respectively (Spencer et al., 2012).

153 The Wash has been heavily influenced by land reclamation since Roman times.
154 Between 1970 and 1980, 800 ha of natural saltmarsh area was reclaimed for
155 agricultural use (Baily and Pearson, 2007) with the last embankment, hereafter
156 referred to as the old seawall, being constructed in 1982. It has been argued that this

157 seawall was constructed too far seaward with the result that the fronting saltmarsh
158 sustained considerable wave erosion (Friess et al., 2014; Symonds and Collins, 2007,
159 2009) and a mean retreat rate of 15 m a^{-1} (Brew and Williams, 2002).

160 The 1996 regional Shoreline Management Plan therefore recommended realignment
161 of this coastal segment (Friess et al., 2008), setting the coastal defence back to an
162 earlier position and allowing for the restoration of formerly reclaimed saltmarshes
163 over an area of 66 ha. Three breaches, each of ca 50 m width, were cut into the old
164 seawall in August 2002 (Figure 1b). An artificial creek system of ca 1200 m in total
165 length was created within the MR and connected to the creek system of the natural
166 saltmarsh in front of the site (Friess et al., 2014; Symonds and Collins, 2007, 2009). It
167 was calculated that the site would inundate fully ca 150 times per year, with 50 %
168 inundation 467 times per year, which would allow for the development of mid to
169 upper marsh communities (just above Mean High Water (MHW)) (Nottage and
170 Robertson, 2005).

171

172 At the time of MR implementation, elevations within the site varied between 2.76 m
173 and 3.33 m ODN (Ordnance Datum Newlyn (where 0.0 m ODN approximates to mean
174 sea level)), allowing for rapid vegetation colonization. By 2006, mean total vegetation
175 cover within the MR was estimated at 86 % (Brown et al., 2007).

176 Over the period November 2002 – April 2008, mean rates of surface elevation changes
177 on natural vegetated saltmarsh control sites (2.91 – 3.40 m ODN), at some distance
178 seaward from the new breaches, showed rates of mean vertical accretion of 0.17 –
179 0.21 cm a^{-1} , comparable to elevation gains seen at other marsh surfaces in the region.

180 Within the MR, one site close to one of the breaches showed an exceptionally high
181 rate of mean surface elevation gain of 18.75 cm in the first 5.5 years after the re-
182 introduction of tidal exchange, one hundred times greater than rates of increase at the
183 control sites (Spencer et al., 2012). This was most likely as a result of high localized
184 sediment supply from breach and channel enlargement and the presence of surfaces
185 left unnaturally low (2.76 – 2.96 m ODN) in the tidal frame as a result of the 1982
186 embanking. By comparison, a site in the middle of the MR (3.11 – 3.23 m ODN) showed
187 a mean elevation gain of 5.19 cm over the same time period but still significantly
188 higher than the external control sites. Finally, sites at the rear of the MR, far from any
189 of the breaches or internal channels, registered rates of mean surface elevation gain of
190 $0.30 - 0.39 \text{ cm a}^{-1}$, only slightly higher than the rates of increase measured at the
191 external control sites (Spencer et al., 2012). The analysis of a LiDAR based digital
192 terrain model from 2016 (provided by the UK Environment Agency) revealed that
193 mean elevation inside the MR ($3.04 \pm 0.42 \text{ m ODN}$) as being higher than that of the
194 adjacent natural marsh ($2.88 \pm 0.5 \text{ m ODN}$).

195

196 *2.2 Water level assessment*

197 Water level measurements were taken at 16 locations in saltmarsh canopies and tidal
198 creeks within the MR scheme of Freiston Shore and in the adjacent natural marsh
199 (Figure 1c). The monitoring period extended over two consecutive springtide periods
200 between 19 September and 12 October 2017. This period coincided with the
201 equinoctial tides, the highest spring tides of the year, which ensured the complete
202 inundation of both the MR site and the natural marshes for several high water events.

203 Hourly meteorological data on wind speeds and direction from Holbeach weather
204 station, 18 km to the south of the study site, were provided by the UK Met Office for
205 the entire monitoring period (Figure 1d).

206 Water levels were recorded with a series of 16 pressure transducers of two types (12
207 Druck PDCR 1830 & 4 Solnist Levellogger Edge Model 3001), both of which have an
208 accuracy of < 1 cm. All sensors were manually calibrated to measure the height of the
209 water column (cm). The measurement interval for the Solnist and Druck sensors was
210 programmed to 30 s and 0.25 s respectively. In order to eliminate the effect of waves
211 on recorded water levels, data from both sensor types were smoothed by calculating
212 moving averages over two minute intervals.

213 The geographic coordinates and elevations of each sensor (Table 1) were determined
214 by a Leica Viva GS08 GNSS satellite survey (RTK) system; all stored measurements were
215 characterised by a 3-D coordinate quality of up to 50 mm, but typically below 20 mm.

216

217

Table 1: Name, coordinates and elevation of each pressure sensor (single-column)

| Sensor # | Latitude | Longitude | Elevation (m ODN) |
|----------|-----------|------------|----------------------|
| Loc 1 | 540724.04 | 343436.682 | 2.99 |
| Loc 2 | 541058.77 | 343224.113 | 2.78 |
| Loc 3 | 541157.14 | 343277.481 | 2.87 |
| Loc 4 | 541671.59 | 343076.004 | 2.08 |
| Loc 5 | 540556.04 | 342136.048 | 1.46 |
| Loc 6 | 540551.82 | 342171.991 | 1.83 |
| Loc 7 | 540546.43 | 342147.882 | 2.58 |
| Loc 8 | 540524.98 | 342149.823 | 2.71 |
| Loc 9 | 540516.16 | 342199.482 | 2.73 |
| Loc 10 | 540724.04 | 343436.682 | 2.99 |
| Loc 11 | 540795.27 | 343379.266 | 2.89 |

| | | | |
|--------|-----------|------------|------|
| Loc 12 | 540764.41 | 343408.975 | 2.9 |
| Loc 13 | 540871.92 | 343290.1 | 3.01 |
| Loc 14 | 540200.98 | 342596.534 | 2.85 |
| Loc 16 | 540248.96 | 342582.824 | 2.19 |
| Loc 17 | 540348.24 | 342583.267 | 1.82 |

218

219 HWL attenuation rates [cm km^{-1}] were calculated from i) the vertical difference in
220 water level between two pressure transducers (termed hereafter as transect), where
221 each pressure transducer represents one location (see Figure 1c) and ii) the measured
222 horizontal distance (m) between the two sensors. Positive rates refer to HWL
223 attenuation, while negative values correspond to an amplification of HWLs along the
224 respective transect. In order to be able to compare HWL attenuation rates across the
225 MR and the natural marsh, but also to account for spatial variabilities within both
226 systems, transects of variable lengths were deployed along four sections (Natural
227 Marsh North (containing 1 transect) & South (3 transects), MR North (7 transects) &
228 South (2 transects) (Figure 1c). This configuration allowed for a comparison of HWL
229 reduction between the MR and the adjacent natural marsh transects.

230 As vegetation properties were considered to be constant during the measurement
231 period, we used water depth and meteorological conditions to explain the event based
232 variability along each transect. The northern (MR North, Natural Marsh North) and
233 southern sections (MR South, Natural Marsh South) (Figure 1c) were more than 1 km
234 apart from each other, which is why we used water depth data from nearby sensors
235 for the respective correlations. For both sections, water depth was taken from the
236 sensor in front of the landward seawall (Loc 1 in the north and Loc 14 in the south)
237 (Figure 1c).

238

239 *2.3 Vegetation survey*

240 Assuming meteorological conditions to be constant across the entire study area,
241 spatial variabilities in HWL attenuation between transects were qualitatively explained
242 by spatial variations in vegetation properties. Vegetation sampling was conducted by
243 following the sampling protocols of Moore (2011); these are consistent with field
244 protocols commonly used in the National Oceanic and Atmospheric Administration's
245 (NOAA) Estuarine Research Reserve Program (Meixler et al., 2018).

246 Vegetation characteristics were recorded next to each pressure sensor location and
247 along each of the four sections (Figure 1c). Species present, and their coverage, height
248 and density, were measured in 39 1 x 1 m quadrats. Two quadrats were measured next
249 to each sensor location. Additional quadrats were selected along all four sections
250 whenever a visible change in the dominant species occurred. Finally, in order to get a
251 representative estimate of the vegetation properties per section (MR North, MR South,
252 Natural Marsh North and Natural Marsh South), density, height and coverage were
253 averaged over the entire section length.

254 The percentage vegetation cover for each species individually, and for the entire
255 quadrat, was visually determined, to the nearest 5%, by comparing the share of
256 vegetation versus remaining bare ground.

257 Vegetation height was assessed for each species by measuring from the substrate to
258 the top of the plant. In order to get a representative estimate of vegetation height per
259 quadrat, this procedure was repeated several times for each species by excluding the

260 highest and lowest 20 % of plants present. The percentage cover and mean vegetation
261 height of each individual species, and the total coverage of the respective quadrat,
262 were used to calculate the mean total vegetation height.

263 Shoot density was determined per species, and for each 1 x 1 m quadrat as a whole, by
264 counting the rooted stems in three 20 x 20 cm sub-quadrats. For *Puccinellia maritima*,
265 which can form very dense carpets in the higher marsh, the frame size was reduced to
266 10 x 10 cm. Finally, mean shoot density was calculated per quadrat using the same
267 procedure as for vegetation height.

268 In addition, to assess the general distribution and coverage of vegetation between
269 sections, a supervised image classification (overall accuracy of 93 %) was conducted for
270 four polygons, each representing one of the four sections. The polygons were created
271 using QGIS software (version 2.18.12), drawing a straight line through each pressure
272 sensor of the respective section and applying a buffer of 50 m around it. The
273 classification used a vertical aerial photograph provided by the UK Environment
274 Agency from 6 May 2016, taken around the time of low water (no aerial photographs
275 were available for 2017). Seasonal differences in vegetation growth between the
276 actual field survey and the aerial photography may have affected vegetation cover
277 estimates. In order to check whether vegetation cover was different between 2016
278 and 2017, the extent and distribution of vegetation, mud and water was compared
279 visually for 12 additional ground reference points (Figure 1c). Subsequently, the
280 proportion of six classes for the areas of interest were assessed: mud, mud with
281 vegetation, water, embankment, vegetation and unclassified.

282

283 *2.4 Statistical analysis*

284 In order to address research question 2, we tested whether or not there was a
285 statistically significant difference in HWL attenuation between the MR site and the
286 adjacent natural marsh over the study period. As the data was neither normally
287 distributed (Shapiro Wilk test p-value < 0.05) nor homoscedastic (Bartlett test p-value
288 < 0.05), a non-parametric Mann Whitney U-test was used.

289 We also tested whether or not HWL attenuation rates inside the MR and in the natural
290 marsh were significantly different from 0. A Shapiro Wilk test confirmed that the data
291 was not normally distributed (MR p-value < 0.0005; Natural Marsh p-value < 0.0005)
292 and thus a non-parametric one-sample Wilcoxon signed rank test was applied to both
293 datasets.

294

295 **3. Results**

296 *3.1 Meteorological conditions*

297 Hourly averaged wind speeds during each high tide's slack water period varied
298 between 7.4 km h⁻¹ and 33 km h⁻¹, with maximum gusts between 11.1 km h⁻¹ and 50.0
299 km h⁻¹. During the measurement period, south-westerly (offshore) winds were
300 dominant, with onshore winds (SSE) only observed during two high water events.
301 During these two events, hourly averaged wind speeds did not exceed 16.7 km h⁻¹.

302

303 3.2 HWL attenuation

304 Overall, the results showed significantly higher (p-value < 0.005) attenuation rates over
 305 the natural marsh, with values ranging between 0 and 101 cm km⁻¹ (mean 46 cm km⁻¹)
 306 compared to the MR, where values ranged from -102 to 160 cm km⁻¹ (mean -3 cm km⁻¹)
 307 ¹) (Table 2).

308 *Table 2: HWL attenuation rates over the Freiston Shore MR, the adjacent natural marsh and the total marsh width.*
 309 *(single-column)*

| Location | Attenuation rate (cm/km) | Length of attenuation (km) |
|-------------------------------|--------------------------|----------------------------|
| Natural Marsh | 0 - 101 | 0.036 - 0.545 |
| MR | -102 - 160 | 0.091 - 0.512 |
| total marsh width (Loc 4 - 1) | 0 - 18 | 1.015 |

310

311 While the results for the natural marsh showed that HWLs were attenuated for all
 312 tides measured, about half of the measurements inside the MR revealed HWLs that
 313 were not attenuated but amplified (Figure 2). In addition, a one-sample Wilcoxon
 314 signed rank test revealed that HWL attenuation rates in the natural marsh were
 315 significantly different from 0 (p-value < 0.005) which was not the case inside the MR
 316 (p-value = 0.5).

317 The differences between the two systems in terms of HWL attenuation are also
318 apparent when looking at the respective standard deviations (Std.). The spread of
319 measured attenuation rates along the individual transects and across the sections (MR

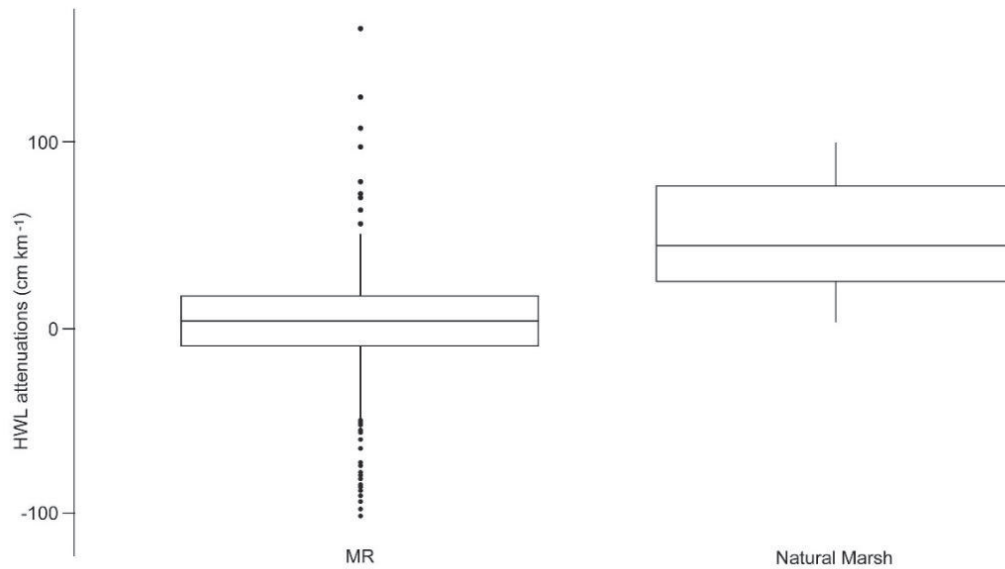


Figure 2: Boxplots of HWL attenuation rates within the Freiston Shore MR site and the adjacent natural marsh. The bottom and top of the box refer to the 25th and 75th percentile, while the centerline constitutes the median. The upper and lower whiskers are calculated as the upper and lower boundary of the box + 1.5 * the inter quartile range. Data points, which did not fall within this range, are plotted as outliers. The results of a non-parametric Mann-Whitney U test revealed that the difference between the MR and the adjacent natural marsh was significant (p -value < 0.0005). (single-column)

320 South, MR North, Natural Marsh South, and Natural Marsh North) revealed
321 considerable temporal and spatial variability (Figure 3).

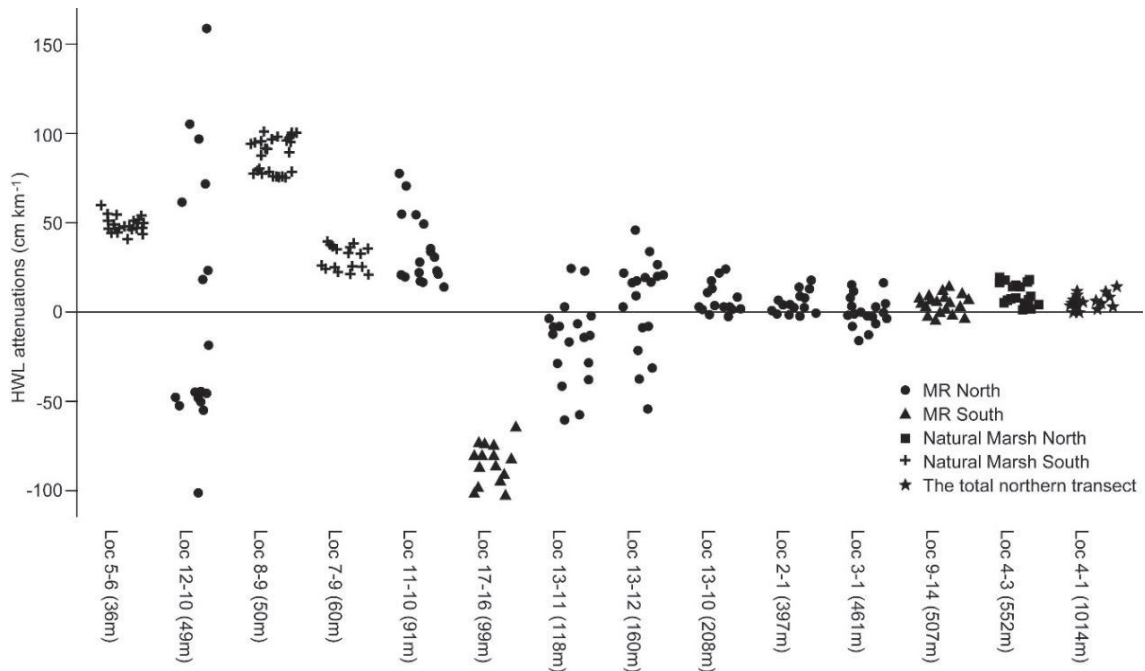


Figure 3: HWL attenuation rates plotted for each location and ordered by transect length. The shape of the data points indicates the respective section. (1.5-column)

322 This variability was found to be exceptionally pronounced inside the MR, where mean
 323 values were considerably higher in the north than in the south (6 cm km^{-1} in the north
 324 and -33 cm km^{-1} in the south), while variability was higher in the south (Std. 44 cm km^{-1}
 325 in the south and 35 cm km^{-1} in the north). In the southern natural marsh, HWL
 326 attenuation rates varied from 23 to 101 cm km^{-1} (mean 56 cm km^{-1} , standard deviation
 327 (Std.) 25 cm km^{-1}); in the northern part of the natural marsh these values were
 328 considerably lower, varying from 0 to 18 cm km^{-1} (mean 9 cm km^{-1} , Std. 6 cm km^{-1}). It
 329 should be noted, however, that values in the northern natural marsh were derived
 330 from only one transect (Loc 4 - 3), whereas measurements in the natural marsh of the
 331 southern section included three transects.

332 The results further indicate that there is a nearly asymptotic relationship between
 333 HWL attenuation and the distance over which the latter was calculated (termed
 334 hereafter as transect length) (Figure 3).

335 The correlation between HWL attenuation and water depth was highly transect
336 specific (Figure 4). In the north, only one transect showed a significantly negative
337 correlation ($R^2 = 0.28$; Figure 4a), but otherwise no significant relationship between
338 HWL attenuation and water depth could be detected, for either the natural marsh or
339 the MR site. In the south, in contrast, the relationship between HWL attenuation and
340 water depth was very different between the MR and the natural marsh (Figure 4b). In
341 the latter, comparatively little variation in HWL attenuation could be explained by
342 water depth ($R^2 = \leq 0.25$), even though two out of three transects still showed a
343 significant correlation (Loc 5 – 6 & Loc 8 – 9). As opposed to the results of the northern
344 section, correlations in the southern natural marsh revealed a positive relationship
345 between the two parameters. Inside the southern MR, significantly negative
346 correlations clarified that most of the variation in HWL attenuation could be explained
347 by water depth ($R^2 = \geq 0.85$; Figure 4b; Loc 9 – 14, Loc 17 – 16).

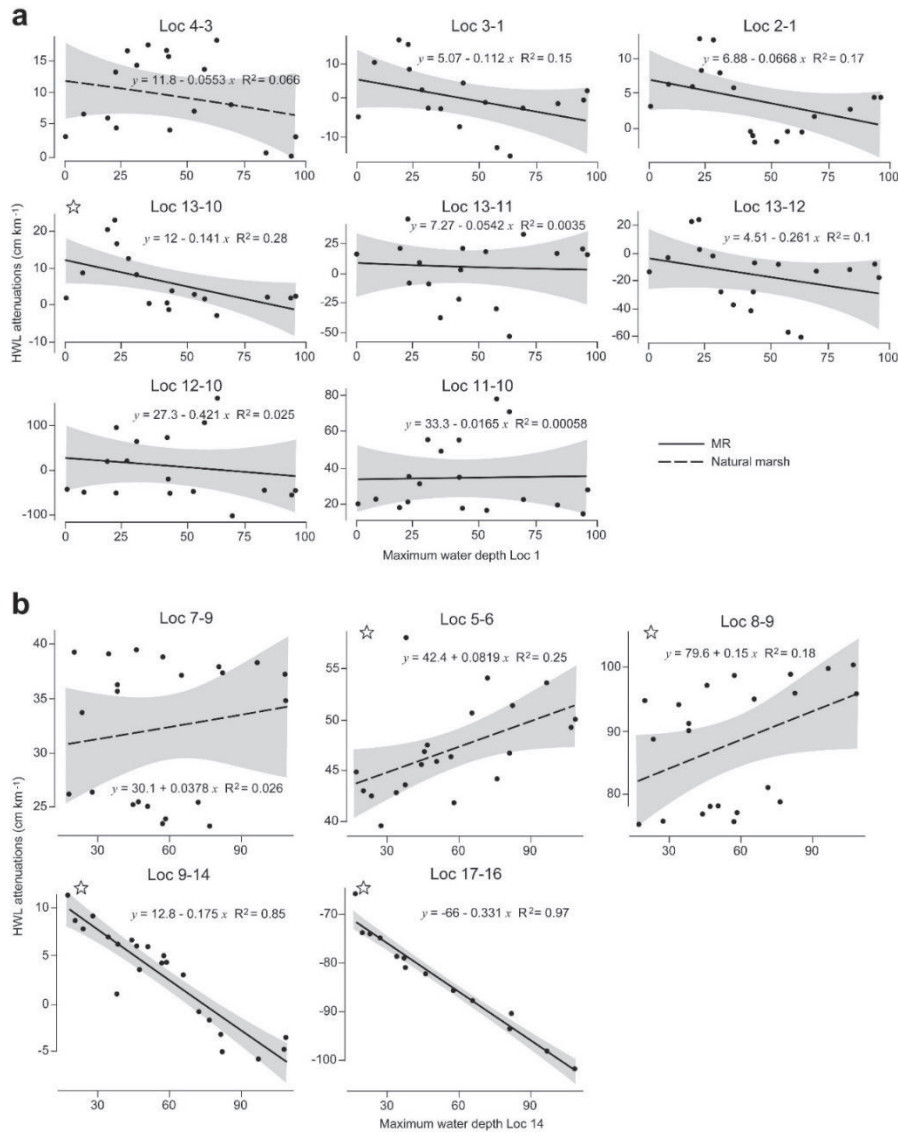


Figure 4a: Scatterplot matrix of HWL attenuation rates for all locations within the northern section and water depth at Loc 1. Shaded areas around the linear models represent the standard deviation and a star indicates significant trends (p -value < 0.05). The p -values for each location were calculated as follows: Loc 4 – 3 = 0.3; Loc 3 – 1 = 0.11; Loc 2 – 1 = 0.088; Loc 13 – 10 = 0.002; Loc 13 – 11 = 0.82; Loc 13 – 12 = 0.19; Loc 12 – 10 = 0.53; Loc 11 – 10 = 0.92

Figure 4b: Scatterplot matrix of HWL attenuation rates for all locations within the southern section and water depth at Loc 14. Shaded areas around the linear models represent the standard deviation and a star indicates significant trends (p -value < 0.05). The p -values for each location were calculated as follows: Loc 7 – 9 = 0.47; Loc 5 – 6 = 0.018; Loc 8 – 9 = 0.049; Loc 9 – 14 < 0.0001 ; Loc 17 – 16 < 0.0001 . (1.5-column)

349 Our results further indicate that besides water depth, wind direction may have
 350 affected HWL attenuation rates and also the observed differences between the MR
 351 and the natural marsh. It is shown that the effect of wind direction is section specific

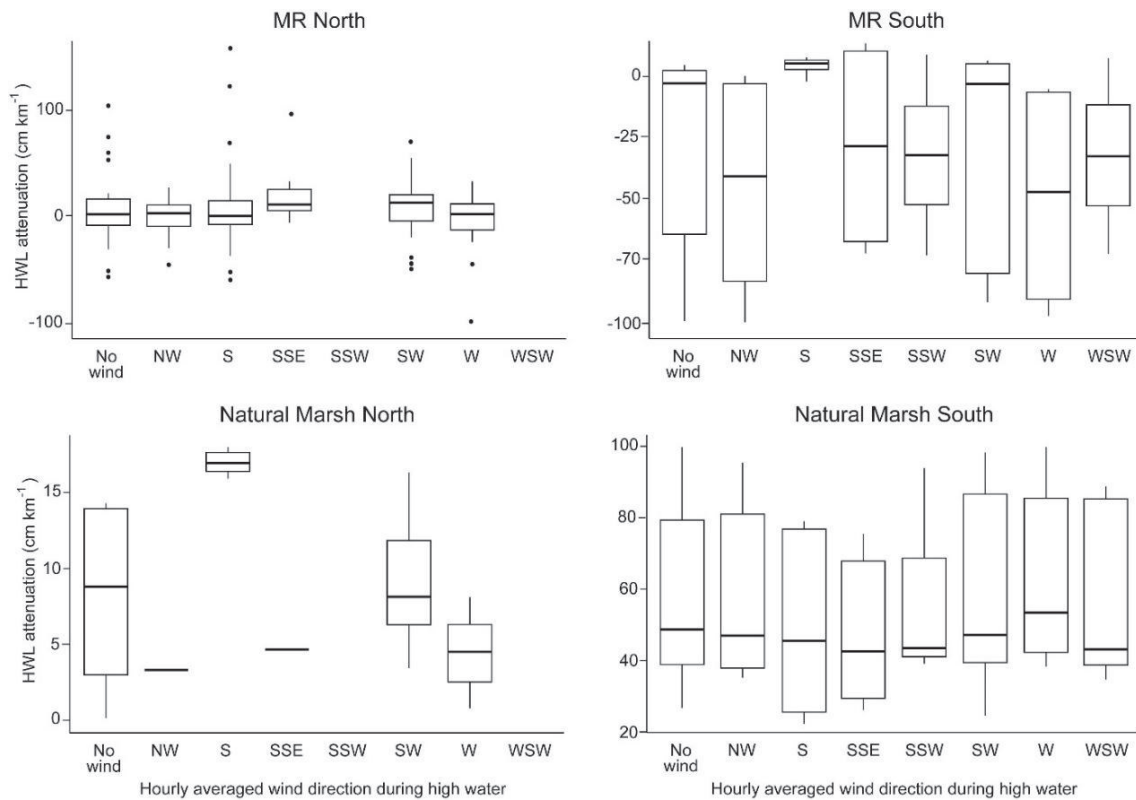


Figure 5: HWL attenuation rates for each section plotted against hourly averaged wind direction during high water slack. Shown are only those tides, where the hourly averaged wind speed during high water slack was $> 11.1 \text{ km h}^{-1}$. The “No Wind” category summarizes attenuation rates for all wind directions, but which were assessed during wind speeds $\leq 11.1 \text{ km h}^{-1}$. The bottom and top of the box refer to the 25th and 75th percentile, while the centerline constitutes the median. The upper and lower whiskers are calculated as the upper and lower boundary of the box $+ 1.5 * \text{the inter quartile range}$. Data points, which did not fall within this range, are plotted as outliers. (1.5-column)

352 (Figure 5). While the southern natural marsh experienced above average rates of HWL
 353 attenuation during northwest (NW; 58 cm km^{-1}), southwest (SW; 59 cm km^{-1}), south-
 354 southwest (SSW; 59 cm km^{-1}) and west (W; 63 cm km^{-1}) winds (compared to an overall
 355 mean attenuation rate of 56 cm km^{-1}), the northern natural marsh showed greater
 356 than average attenuation only under southerly (S; 17 cm km^{-1}) winds (compared to an
 357 overall mean of 9 cm km^{-1}). The northern MR exhibited low rates of HWL attenuation

358 and even amplification during NW (-1 cm km^{-1}), W (-5 cm km^{-1}) and WNW (-3 cm km^{-1})
359 winds (compared to an overall mean of 6 cm km^{-1}). HWL amplification inside the
360 southern MR predominantly occurred during NW (-46 cm km^{-1}), SW (-36 cm km^{-1}) and
361 W (-50 cm km^{-1}) winds (compared to an overall mean of -33 cm km^{-1}). In summary,
362 while westerly and north-westerly winds were more likely to result in above average
363 HWL attenuation in the southern natural marsh, they had the opposite effect inside
364 both sections of the MR.

365

366 *3.3 Vegetation characteristics*

367 The locations with highest mean vegetation height in the southern natural marsh (43.5
368 cm) clearly coincided with those transects over which the highest HWL attenuation
369 rates were observed during this study. However, spatial variations in HWL attenuation
370 along the other sections could not be explained by differences in vegetation properties
371 (Figure 6). For example, highest shoot densities were measured in the northern and
372 southern MR ($1755 \text{ stems m}^{-2}$ and $1121 \text{ stems m}^{-2}$), while values in the natural marshes
373 were significantly lower, with 287 stems m^{-2} in the northern and $224 \text{ stems per m}^{-2}$ in
374 the southern natural marsh. These differences likely appeared due to the locally high
375 abundances of the common saltmarsh-grass *Puccinellia maritima*. Whilst HWL
376 attenuation was higher in the northern MR compared to the southern MR, in
377 accordance with the higher stem density, it was generally significantly less than that
378 recorded in the natural marsh, despite the much lower stem densities.

379

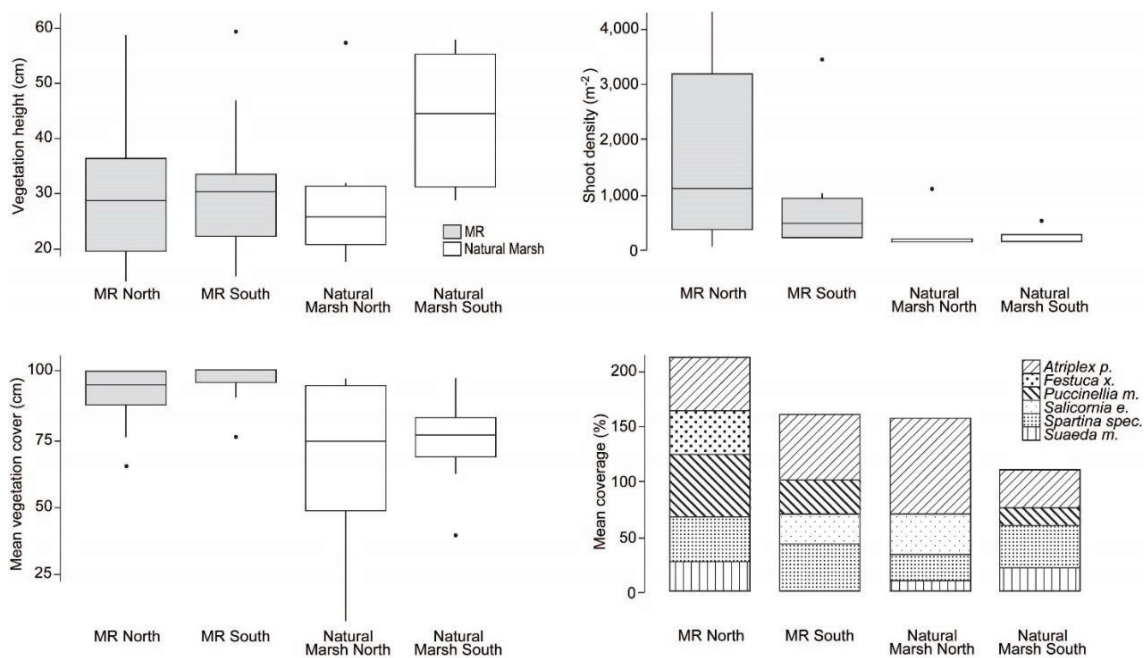


Figure 6: Vegetation characteristics and species per section. Only those genera are shown for which coverage exceeded 10 %. (1.5-column)

380 Furthermore, differences in vegetation cover among the sampled quadrats did not
 381 explain the differences in HWL attenuation between the sections. Similar to shoot
 382 densities, mean vegetation cover of sampled plots inside the MR (MR North 92 % and
 383 MR South 96 %) was higher compared to the southern (74 %) and northern natural
 384 marsh (67 %). However, the assessment of vegetation cover by means of the
 385 supervised image classification (not represented in the field measurements shown in
 386 Figure 6) showed that vegetation cover was highest in the southern natural marsh (90
 387 %), coinciding with the tallest vegetation (Fig. 6) and highest HWL attenuation rates.
 388 The second highest vegetation cover was measured in the northern MR (81 %), while
 389 the northern natural marsh (74 %) and the southern MR (73 %) showed very similar
 390 cover characteristics. The lower vegetation cover in the northern natural marsh
 391 compared to the southern natural marsh may be the result of the high proportion of
 392 dissecting tidal creeks, as reflected in the high share of area classified as mud (9 %

393 compared to 5 % Natural Marsh South; 6 % MR South & 7 % MR North). The
394 percentage of open water areas was higher inside the MR compared to the natural
395 marsh (9 % MR North; 10 % MR South; 1 % Natural Marsh North; < 1 % Natural Marsh
396 South), reflecting both the artificial internal creek system and a high surface coverage
397 of waterlogged areas and bare pools.

398

399 **4. Discussion**

400 *4.1 Has managed realignment led to a reduction in HWLs at the landward margin of*
401 *the realignment site and how variable is HWL attenuation across space and*
402 *time within this MR site?*

403 The results of this study show that, for the conditions encountered during the field
404 monitoring period, the capacity of the Freiston Shore MR site to provide HWL
405 attenuation was limited. In fact, HWL attenuation rates inside the MR were not
406 significantly different from zero. This was unexpected as the site exhibits high bed
407 friction, due to its extensive vegetation cover and (artificial) topographic complexity
408 resulting from the presence of excavated channels and constructed surface mounds
409 and hollows. These results and the large HWL attenuation range observed inside the
410 MR suggest that the existing relationship between HWL attenuation and bottom
411 friction is more complex, as previously suggested by Resio and Westerink (2008) and
412 that the effects of vegetation on surge height reduction cannot be combined to a
413 “single reduction factor” (Reed et al., 2018). This may be particularly valid in smaller
414 enclosed basins such as MR sites. Rather, the comparatively high spatial (between

415 transects) and event driven variability of HWL attenuation inside the scheme (Figure
416 3), indicate that internal hydrodynamics, resulting from the combined effects of
417 variations in water depth and meteorological forcing, may have counteracted the
418 attenuation of water levels induced by the additional shallow water area provided by
419 the restored saltmarsh.

420 This reasoning is supported by differences in the correlation between HWL attenuation
421 and water depth between the southern MR site and the adjacent natural marsh. Inside
422 the MR, correlations were significantly negative, while relations were positive in the
423 adjacent natural marsh (Figure 4b). This indicates that for the inundation depths
424 encountered during the monitoring period (varying between 16 – 110 cm at Loc 14),
425 the southern natural marsh did not reach its full HWL attenuation potential. On the
426 other hand, the same inundation depths were found to cause HWL amplification inside
427 the southern MR. The occurrence of HWL amplification under comparatively low
428 inundation depths may compromise the performance of the MR site under increasing
429 inundation depths, for example during event-based storm surge conditions or, in the
430 long term, with respect to sea level rise. Stark et al. (2015) argued that the ideal
431 inundation depth range for marshes to reach their highest attenuation rates lies
432 between 0.5 – 1.0 m. At Freiston, this claim works well for the natural marsh, but not
433 at all for the MR.

434

435 4.2 For a specific range of tidal inundations, can a demonstrable difference be seen
 436 in HWL attenuation between the MR scheme and the adjacent natural
 437 saltmarsh?

438 The results of this study suggest considerably higher HWL attenuation rates over the
 439 natural marsh, than previously measured in the field (Table 3) and significantly higher
 440 than measurements inside the MR site. It can be argued that the high capacity of the
 441 natural marsh to reduce maximum water levels is a result of two factors. Firstly, during
 442 27 % of the-high tide slack water periods assessed, the wind direction was southwest
 443 (i.e. offshore), a direction that was found to result in the highest HWL attenuation over
 444 the natural marsh (Figure 5).

445 *Table 3: Observed attenuation rates in wetlands from previous field studies. Adapted from Stark et al., (2015) and*
 446 *Paquier et al., (2016). (1.5-column)*

| Location | Description | Attenuation rate (cm/km) | Length of attenuation (km) | Reference |
|---|---|--------------------------|----------------------------|---|
| Louisiana | Hurricane Andrew (1992) surge reduction over 37 km of marsh and open water | 4.4 - 4.9 | 37 | Lovelace (1994), Wamsley et al., (2010) |
| Great Marshes, Massachusetts | Mean HWL variation across tidal flats and saltmarsh channels | -2 - 11 | / | Calculated by Stark et al., (2015) from figures in Van der Molen (1997) |
| Ten thousand islands, National Wildlife Refuge, Florida | Hurricane Charley (2004) surge reduction across 5.5 km of marshes and mangroves | 9.4 - 15.8 | 5.5 | Krauss et al., (2009) |
| Shark River (Everglades), Florida | Hurricane Wilma (2005) surge reduction over 14 km of riverine mangrove | 4.0 - 6.9 | 14 | Krauss et al., (2009) |
| Cameron Prairie, Louisiana | Hurricane Rita (2005) surge reduction in marsh area | 10.0 | / | McGee et al., (2006), Wamsley et al., (2010) |
| Sabine, Louisiana | Hurricane Rita (2005) surge reduction in marsh area | 25.0 | / | McGee et al., (2006), Wamsley et al., (2010) |

| | | | | |
|---|---|------------|------|--|
| Vermillion, Louisiana | Hurricane Rita (2005) surge reduction in marsh area | 4.0 | / | McGee et al., (2006), Wamsley et al., (2010) |
| Vermillion, Louisiana | Hurricane Rita (2005) surge reduction in marsh area | 7.7 | / | McGee et al., (2006), Wamsley et al., (2010) |
| Western Scheldt estuary, Saeftinghe Marsh | Regular Spring to Neap tides including two storm surge events over saltmarsh surfaces and within tidal channels | -2 - 70 | / | Stark et al., (2015), evaluated from figures |
| Chesapeake Bay | Measured over tides and two storm surge events | -280 - 270 | 0.02 | Paquier et al., (2016) |

447 Secondly, the most extreme HWL attenuation rates were measured along the shortest
448 transects (Figure 3). Three out of four transects in the natural marsh were measured
449 over comparatively short distances of less than 60 m. Previously, similar rates have
450 only been measured by Paquier et al. (2017) and by Stark et al. (2015), also over very
451 short vegetated marsh platform transects (Table 3). Two possible explanations for this
452 phenomenon can be found in the literature. Firstly, the flow field over vegetated
453 surfaces is dominated by high friction induced by the presence of vegetation (Stark et
454 al., 2015; van Oyen et al., 2012; van Oyen et al., 2014). This friction is reduced over
455 longer transects, which typically include areas of high density vegetation canopies but
456 also mud, standing water and low and pioneer communities with widely spaced
457 individual plant stems. Secondly, HWL attenuation is not a linear process. Rather, it is
458 spatially highly variable, depending on local marsh morphology, vegetation and
459 hydrodynamic forcing (Resio and Westerink, 2008; Stark et al., 2016; Temmerman et
460 al., 2012). These arguments are supported by this study, where highest attenuation
461 rates were observed along short transects in the southern natural marsh. These were
462 also transects where vegetation height and cover were highest. Thus short transects
463 over saltmarsh surfaces may generate maximum (within highly vegetated marsh

464 transect) or minimum friction (on bare sediments) on the water column, depending on
465 the surface cover and topography. This effect is averaged over the entire marsh width,
466 resulting in converging HWL attenuation rates when measured over longer distances.

467 The exceptionally high attenuation rates across the natural marsh alone, however, do
468 not explain the discrepancies with respect to the MR site. The weak performance of
469 the MR site may originate from differences in those saltmarsh characteristics which are
470 known to determine HWL attenuation. It is well known that the effectiveness of
471 wetlands in attenuating HWLs is dependent upon regional and local bathymetry,
472 including the height, width and topography of fronting mudflats and sandflats; on local
473 surface geometry and raised-feature elevations (Resio and Westerink, 2008); the
474 presence of a closed vegetation cover of high and flexible stems (Resio and Westerink,
475 2008; Rupprecht et al., 2017); and the interaction of shallow water flows with a tidal
476 creek network (Resio and Westerink, 2008; Smolders et al., 2015; Stark et al., 2015;
477 Stark et al., 2016; Temmerman et al., 2012). By analysing 19 MR sites (including
478 Freiston Shore), Lawrence et al. (2018) found that restored saltmarshes lack the
479 variations in topographic roughness found in natural marshes. Marsh topography
480 affects vegetation development (Lawrence et al., 2018), which helps to explain why
481 vegetation characteristics of MR sites established on agricultural soils, such as Freiston
482 Shore, differ from those of natural marshes (Mossman et al., 2012). Furthermore, a
483 patchy vegetation cover, as found inside the Freiston Shore MR, considerably reduces
484 HWL attenuation rates (Temmerman et al., 2012). Based on the interrelation between
485 morphology, vegetation and HWL attenuation, the restoration of a naturally complex
486 and diverse topography should be a key objective of future MR schemes. However, the

487 effects of morphologic complexity (including rugosity, topographic wetness, surface
 488 curvature and distance to creek (Lawrence et al., 2018)) on HWL attenuation rates
 489 have not yet been quantified (Möller and Christie, 2018). The detailed understanding
 490 of these controls on HWL attenuation is crucial for enhancing the future performance
 491 of similar saltmarsh restoration schemes.

492

493 *4.3 Managed Realignment: scheme design, meteorological forcing and HWL*
 494 *attenuation*

495 The relative importance of meteorological conditions to spatial patterns of water levels
 496 within the MR site may be related to the design of the MR scheme. This is likely to be
 497 particularly significant where seawall breaches have been used as the means of re-
 498 establishing tidal exchange and thus much of the seawall perimeter to the site remains
 499 intact. Previous studies in natural marshes have shown that storage area limitations

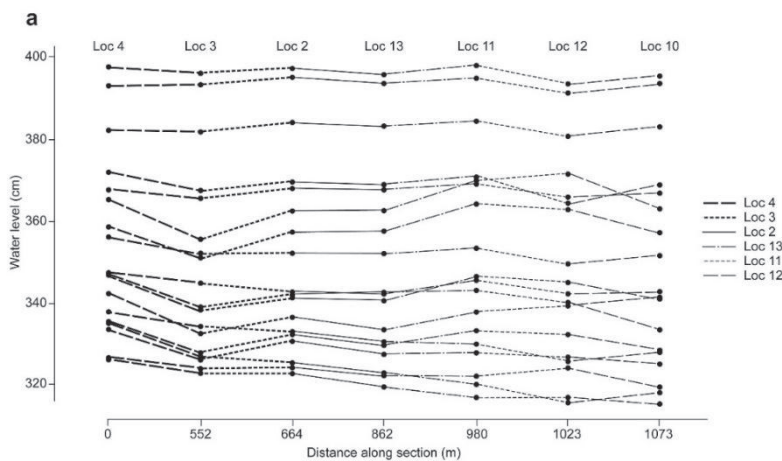


Figure 7a: Cross section of water levels for both northern sections (including Natural Marsh North and MR North). Water levels are plotted for every sensor (shape) and every tide (line) on the y-axis, while distance is placed on the x-axis and measured in m from the most seaward sensor (Loc 4) in landward direction.

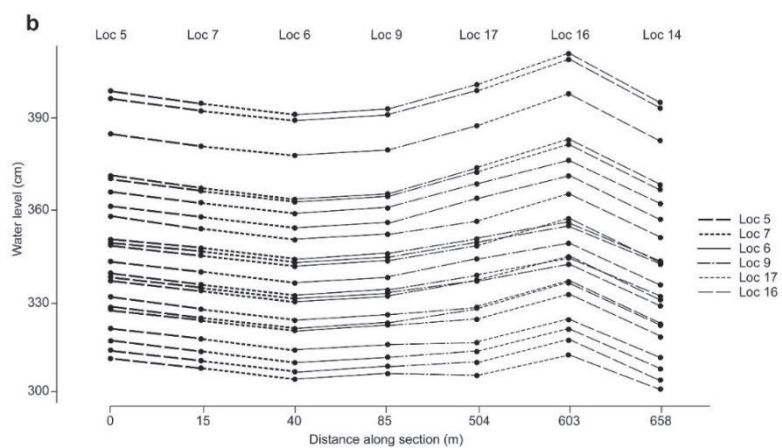


Figure 7b: Cross section of water levels for both southern sections (including Natural Marsh South and MR South). Water levels are plotted for every sensor (shape) and every tide (line) on the y-axis, while distance is placed on the x-axis and measured in m from the most seaward sensor (Loc 5) in landward direction. (1.5-column)

500 for flood waters, for example, may cause water blockage against dikes or other
501 structures confining the marsh size, causing HWL amplification (Stark et al., 2016). The
502 results from Freiston support this observation. The positioning of the seawall
503 boundaries to the MR site relative to tidally and meteorologically forced water levels
504 led to HWL amplification over the study period (Figure 7a: Loc 12 - 10 ; Figure 7b: Loc 6
505 – 9 and over the course of the MR, peaking at Loc 16). Resio et al. (2008) further
506 explain this phenomenon; HWL amplification by water blockage occurs when the
507 duration of the hydrodynamic forcing is long compared to the time it takes to fill the
508 storage area. Here we further suggest that this effect may be amplified by
509 meteorological conditions. Consequently, the size of a MR is an important factor in
510 determining whether or not a created, or recreated, saltmarsh can reach its full
511 attenuation capacity. This constitutes a true wetland restoration dilemma, as site size
512 is often a major limiting factor towards MR implementation. In 2013, 66 % of MR sites
513 in England were smaller than 20 ha (Esteves, 2013). In addition, this finding raises
514 questions regarding the performance of the already existing MR schemes across the
515 UK, which are mostly smaller than Freiston Shore (66 ha), with a mean size of currently
516 48 ha (Boorman and Hazelden, 2017).

517 Inside the MR, prevailing westerly and south-westerly winds were found to result in
518 exceptionally low rates of HWL attenuation inside the MR. We suspect that the effect
519 of wind drag is greater on an almost enclosed body of water than for an open body of
520 water, such as encountered outside the MR in the natural marsh. This effect may be
521 amplified when wind speeds exceed those encountered during our monitoring period.
522 It is clear that scheme design is likely to have considerable implications for the

523 potential of any MR to reduce maximum water levels. Yet problematically, in many
524 cases, constraints around land ownership and availability will most likely leave little
525 choice regarding the actual location or orientation of the MR. These findings may also
526 revive the debate on whether to perform bank removal or breach restoration, which
527 has been termed “one of the unresolved problems facing the UK intertidal restoration
528 program” (Pethick, 2002, 434).

529 Extensive application of nature-based coastal defences is still hampered by a lack of
530 knowledge regarding their performance in terms of reducing the risk of coastal
531 flooding, as well as by a general lack of comprehensive design guidelines (Bouma et al.,
532 2014; Reed et al., 2018). In establishing these guidelines, adequate consideration of
533 the effects of site geometry, meteorological conditions, and restored surface
534 characteristics on site internal hydrodynamics is urgently required.

535

536 **Conclusions**

537 For the conditions encountered during the field monitoring period, the capacity of the
538 Freiston Shore MR site to provide HWL attenuation was limited. HWL attenuation rates
539 were significantly higher in the natural saltmarsh (in front of the MR), where HWL
540 attenuation ranged between 0 and 101 cm km⁻¹ (mean 46 cm km⁻¹). Within the MR
541 site, rates varied between -102 and 160 cm km⁻¹ (mean -3 cm km⁻¹), with even negative
542 attenuation (i.e. amplification) for about half of the measured tides.

543 The weak performance of the MR site in terms of HWL attenuation was a result of
544 internal hydrodynamics caused by scheme design and meteorological conditions,

545 counteracting the HWL attenuating effect caused by the additional shallow water area
546 provided by the restored saltmarsh.

547 The findings of this study make clear that current design, monitoring and assessment
548 approaches at MR sites may result in unrealized (HWL attenuation) potential (Spencer
549 and Harvey, 2012). In order to fully exploit this potential in future MR schemes,
550 forthcoming research should examine more closely the driving forces of HWL
551 attenuation in space (site geometry and orientation, surface morphology, tidal creek
552 network characteristics, vegetation canopy types and their site coverage) and time
553 (wind strength, duration and direction and associated wave fields and water depths).
554 The results of such studies should then be used to establish better guidelines for MR
555 scheme design and implementation, to result in more effective HWL attenuation.

556 This in turn should enable the wider implementation of managed realignment at the
557 coast, by fostering stronger, scientific evidence-based coastal management and public
558 support and confidence.

559

560 **Acknowledgements**

561 JK thanks the German Academic Exchange Service (Grant ID 57314604) and the Future
562 Ocean Excellence Cluster (University of Kiel) for funding his stay in Cambridge, as a
563 member of the Department of Geography's Visiting Scholar Programme. We thank B.
564 Evans and E. Christie, Cambridge Coastal Research Unit, for technical and field
565 assistance.

566 The authors thank the Royal Society for the Protection of Birds, for access for research
567 at the Freiston Shore reserve and the UK Environment Agency, for the supply of
568 vertical aerial photography and LiDAR data.

569

570 References

571 Associated British Ports Marine Environmental Research (ABPmer), 2010. The online managed
572 realignment guide. ABPmer. <http://www.abpmer.net/omreg/>. Accessed 04.15.2018.

573 Baily, B., Pearson, A.W., 2007. Change Detection Mapping and Analysis of Salt Marsh Areas of
574 Central Southern England from Hurst Castle Spit to Pagham Harbour. *J. Coastal Res.* 23 (6),
575 1549–1564.

576 Boorman, L.A., Hazelden, J., 2017. Managed re-alignment; a salt marsh dilemma? *Wetl. Ecol.*
577 *Manag.* 25 (4), 387–403.

578 Bouma, T.J., van Belzen, J., Balke, T., Zhu, Z., Airoidi, L., Blight, A.J., Davies, A.J., Galvan, C.,
579 Hawkins, S.J., Hoggart, S.P., Lara, J.L., Losada, I.J., Maza, M., Ondiviela, B., Skov, M.W.,
580 Strain, E.M., Thompson, R.C., Yang, S., Zanuttigh, B., Zhang, L., Herman, P.M., 2014.

581 Identifying knowledge gaps hampering application of intertidal habitats in coastal
582 protection: Opportunities & steps to take. *Coast. Eng.* 87, 147–157.

583 Brew, D.S., Williams, A., 2002. Shoreline Movement and Shoreline Management in The Wash,
584 Eastern England. *Littoral Conference 2002, the changing coast, Porto, Portugal*, 313–320.

585 Brown, S.L., Pinder, A., Scott, L., Bass, J., Rispin, E., Brown, S., Garbutt, A., Thomson, A.,
586 Spencer, T., Möller, I., Brooks, S.M., 2007. Wash banks flood defence scheme Freiston
587 environment monitoring 2002 - 2006. FD 1911/TR. Joint DEFRA/EA Flood and Coastal
588 Erosion Risk Management R&D Programme.

589 Church, J.A., Clark, P.U., Cazenave, A., Gregory, J.M., Jevrejeva, S., Levermann, A., Merrifield,
590 M.A., Milne, G.A., 2013. Sea Level Change, in: Stocker, T.F., Quin, D., Plattner, G.-K., Tignor,
591 M., Allen, S.K., Boschung, J., Nauels, A., Xia, Y., Bex, V., Midgley, P.M. (Eds.), Climate
592 Change 2013: The Physical Science Basis. Contribution of Working Group I to the Fifth
593 Assessment Report of the Intergovernmental Panel on Climate Change, Cambridge, United
594 Kingdom and New York, NY, USA.

595 Committee on Climate Change, 2013. Managing the land in a changing climate. Chapter 5:
596 Regulating services - coastal habitats. [https://www.theccc.org.uk/wp-](https://www.theccc.org.uk/wp-content/uploads/2013/07/ASC-2013-Book-singles_2.pdf)
597 [content/uploads/2013/07/ASC-2013-Book-singles_2.pdf](https://www.theccc.org.uk/wp-content/uploads/2013/07/ASC-2013-Book-singles_2.pdf). Accessed 10 April 2018.

598 Cooper, J., McKenna, J., 2008. Working with natural processes: the challenge for coastal
599 protection strategies. *Geogr. J.* 174 (4), 315–331.

600 Dixon, A.M., Leggett, D.J., Weight, R.C., 1998. Habitat Creation Opportunities for Landward
601 Coastal Re-alignment: Essex Case Studies. *Water Environ. J.* 12 (2), 107–112.

602 Esteves, L.S., 2013. Is managed realignment a sustainable long-term coastal management
603 approach? *J. Coastal Res.* SI65, 933–938.

604 Esteves, L.S., Thomas, K., 2014. Managed realignment in practice in the UK: Results from two
605 independent surveys. *J. Coastal Res.* SI70, 407–413.

606 Friess, D., Möller, I., Spencer, T., 2008. Managed realignment and the re-establishment of
607 saltmarsh habitat, Freiston Shore, Lincolnshire, United Kingdom, in: , *The Role of*
608 *Environmental Management and Eco-Engineering in Disaster Risk Reduction and Climate*
609 *Change Adaptation*, pp. 65–78.

610 Friess, D.A., Möller, I., Spencer, T., Smith, G.M., Thomson, A.G., Hill, R.A., 2014. Coastal
611 saltmarsh managed realignment drives rapid breach inlet and external creek evolution,
612 Freiston Shore (UK). *Geomorphology* 208, 22–33.

613 Garbutt, R.A., Reading, C.J., Wolters, M., Gray, A.J., Rothery, P., 2006. Monitoring the
614 development of intertidal habitats on former agricultural land after the managed
615 realignment of coastal defences at Tollesbury, Essex, UK. *Mar. Pollut. Bull.* 53 (1-4), 155–
616 164.

617 Kirwan, M.L., Temmerman, S., Skeehan, E.E., Guntenspergen, G.R., Fagherazzi, S., 2016.
618 Overestimation of marsh vulnerability to sea level rise. *Nat. Clim. Change* 6 (3), 253–260.

619 Knutson, P.L., Seeling, W.N., Inskeep, M.R., 1982. Wave dampening in *Spartina alterniflora*
620 marshes. *Wetlands* 2 (1), 87–104.

621 Knutson, T.R., McBride, J.L., Chan, J., Emanuel, K., Holland, G., Landsea, C., Held, I., Kossin, J.P.,
622 Srivastava, A.K., Sugi, M., 2010. Tropical cyclones and climate change. *Nat. Geosci.* 3, 157–
623 163.

624 Lawrence, P.J., Smith, G.R., Sullivan, M.J., Mossman, H.L., 2018. Restored saltmarshes lack the
625 topographic diversity found in natural habitat. *Ecol. Eng.* 115, 58–66.

626 Leonardi, N., Carnacina, I., Donatelli, C., Ganju, N.K., Plater, A.J., Schuerch, M., Temmerman, S.,
627 2018. Dynamic interactions between coastal storms and salt marshes: A review.
628 *Geomorphology* 301, 92–107.

629 Loder, N.M., Irish, J.L., Cialone, M.A., Wamsley, T.V., 2009. Sensitivity of hurricane surge to
630 morphological parameters of coastal wetlands. *Estuar. Coast. Shelf Sci.* 84 (4), 625–636.

631 Mazik, K., Musk, W., Dawes, O., Solyanko, K., Brown, S., Mander, L., Elliott, M., 2010. Managed
632 realignment as compensation for the loss of intertidal mudflat: A short term solution to a
633 long term problem? *Estuar. Coast. Shelf Sci.* 90 (1), 11–20.

634 Meixler, M.S., Kennish, M.J., Crowley, K.F., 2018. Assessment of Plant Community
635 Characteristics in Natural and Human-Altered Coastal Marsh Ecosystems. *Estuaries Coast.*
636 41 (1), 52–64.

637 Möller, I., Christie, E., 2018. Hydrodynamics and Modeling of Water Flow in Coastal Wetlands,
638 in: Perillo, G.M.E., Wolanski, E., Cahoon, D.R., Hopkinson, C.S. (Eds.), Coastal wetlands. An
639 integrated ecosystem approach, 2nd edition ed. Elsevier, Amsterdam.

640 Möller, I., Kudella, M., Rupprecht, F., Spencer, T., Paul, M., van Wesenbeeck, B.K., Wolters, G.,
641 Jensen, K., Bouma, T.J., Miranda-Lange, M., Schimmels, S., 2014. Wave attenuation over
642 coastal salt marshes under storm surge conditions. *Nat. Geosci.* 7 (10), 727–731.

643 Möller, I., Spencer, T., French, J.R., Leggett, D.J., Dixon, M., 1999. Wave Transformation Over
644 Salt Marshes: A Field and Numerical Modelling Study from North Norfolk, England. *Estuar.
645 Coast. Shelf Sci.* 49 (3), 411–426.

646 Moore, K., 2011. NERRS SWMP biomonitoring protocol: long-term monitoring of estuarine
647 submersed and emergent vegetation communities. Technical Report Series. NOAA, Silver
648 Spring, 14 pp.

649 Mossman, H.L., Davy, A.J., Grant, A., 2012. Does managed coastal realignment create
650 saltmarshes with ‘equivalent biological characteristics’ to natural reference sites? *J. Appl.
651 Ecol.* 49 (6), 1446–1456.

652 Nerem, R.S., Beckley, B.D., Fasullo, J.T., Hamlington, B.D., Masters, D., Mitchum, G.T., 2018.
653 Climate-change-driven accelerated sea-level rise detected in the altimeter era. *Proc. Natl.
654 Acad. Sci. U.S.A.* 115 (9), 2022–2025.

655 Nottage, A., Robertson, P., 2005. The saltmarsh creation handbook: A project manager's guide
656 to the creation of saltmarsh and intertidal mudflat / by Albert Nottage and Peter
657 Robertson. Royal Society for the Protection of Birds, Sandy.

658 Paquier, A.-E., Haddad, J., Lawler, S., Ferreira, C.M., 2017. Quantification of the Attenuation of
659 Storm Surge Components by a Coastal Wetland of the US Mid Atlantic. *Estuaries Coast.* 40
660 (4), 930–946.

661 Pethick, J., 2002. Estuarine and Tidal Wetland Restoration in the United Kingdom: Policy Versus
662 Practice. *Restoration Ecol.* 10 (3), 431–437.

663 Pye, K., 1995. Controls on Long-term Saltmarsh Accretion and Erosion in the Wash, Eastern
664 England. *J. Coastal Res.* 11 (2), 337–356.

665 Reed, D., van Wesenbeeck, B., Herman, P.M., Meselhe, E., 2018. Tidal flat-wetland systems as
666 flood defenses: Understanding biogeomorphic controls. *Estuar. Coast. Shelf Sci.* 213, 269–
667 282.

668 Resio, D.T., Westerink, J.J., 2008. Modeling the physics of storm surges. *Phys. Today* 61 (9), 33–
669 38.

670 Rupprecht, F., Möller, I., Paul, M., Kudella, M., Spencer, T., van Wesenbeeck, B.K., Wolters, G.,
671 Jensen, K., Bouma, T.J., Miranda-Lange, M., Schimmels, S., 2017. Vegetation-wave
672 interactions in salt marshes under storm surge conditions. *Ecol. Eng.* 100, 301–315.

673 Schuerch, M., Spencer, T., Temmerman, S., Kirwan, M.L., Wolff, C., Lincke, D., McOwen, C.J.,
674 Pickering, M.D., Reef, R., Vafeidis, A.T., Hinkel, J., Nicholls, R.J., Brown, S., 2018. Future
675 response of global coastal wetlands to sea-level rise. *Nature* 561, 231–234.

676 Shepard, C.C., Crain, C.M., Beck, M.W., 2011. The protective role of coastal marshes: a
677 systematic review and meta-analysis. *PloS one* 6 (11), e27374.

678 Smolders, S., Plancke, Y., Ides, S., Meire, P., Temmerman, S., 2015. Role of intertidal wetlands
679 for tidal and storm tide attenuation along a confined estuary: A model study. *Nat. hazards*
680 *earth syst. sci.* 15 (7), 1659–1675.

681 Spencer, K.L., Harvey, G.L., 2012. Understanding system disturbance and ecosystem services in
682 restored saltmarshes: Integrating physical and biogeochemical processes. *Estuar. Coast.*
683 *Shelf Sci.* 106, 23–32.

684 Spencer, T., Friess, D.A., Möller, I., Brown, S.L., Garbutt, R.A., French, J.R., 2012. Surface
685 elevation change in natural and re-created intertidal habitats, eastern England, UK, with
686 particular reference to Freiston Shore. *Wetl. Ecol. Manag.* 20 (1), 9–33.

687 Stark, J., Plancke, Y., Ides, S., Meire, P., Temmerman, S., 2016. Coastal flood protection by a
688 combined nature-based and engineering approach: Modeling the effects of marsh
689 geometry and surrounding dikes. *Estuar. Coast. Shelf Sci.* 175, 34–45.

690 Stark, J., van Oyen, T., Meire, P., Temmerman, S., 2015. Observations of tidal and storm surge
691 attenuation in a large tidal marsh. *Limnol. Oceanogr.* 60 (4), 1371–1381.

692 Symonds, A.M., Collins, M.B., 2007. The development of artificially created breaches in an
693 embankment as part of a managed realignment, Freiston Shore, UK. *J. Coastal Res.* SI50,
694 130–134.

695 Symonds, A.M., Collins, M.B., 2009. Sediment dynamics associated with managed realignment:
696 Freiston Shore, The Wash, UK, in: *Proceedings of the 29th International Conference,*
697 *National Civil Engineering Laboratory, Lisbon, Portugal. 19 – 24 September 2004*, pp. 3173–
698 3185.

699 Syvitski, J.P.M., Kettner, A.J., Overeem, I., Hutton, E.W.H., Hannon, M.T., Brakenridge, G.R.,
700 Day, J., Vörösmarty, C., Saito, Y., Giosan, L., Nicholls, R.J., 2009. Sinking deltas due to
701 human activities. *Nat. Geosci.* 2 (10), 681–686.

702 Temmerman, S., Meire, P., Bouma, T.J., Herman, P.M.J., Ysebaert, T., Vriend, H.J. de, 2013.
703 Ecosystem-based coastal defence in the face of global change. *Nature* 504, 79–83.

704 Temmerman, S., Vries, M.B. de, Bouma, T.J., 2012. Coastal marsh die-off and reduced
705 attenuation of coastal floods: A model analysis. *Glob. Planet. Change* 92–93, 267–274.

706 Tempest, J.A., Möller, I., Spencer, T., 2015. A review of plant-flow interactions on salt marshes:
707 The importance of vegetation structure and plant mechanical characteristics. *WIREs Water*
708 2 (6), 669–681.

709 Thorslund, J., Jarsjo, J., Jaramillo, F., Jawitz, J.W., Manzoni, S., Basu, N.B., Chalov, S.R., Cohen,
710 M.J., Creed, I.F., Goldenberg, R., Hylin, A., Kalantari, Z., Koussis, A.D., Lyon, S.W., Mazi, K.,
711 Mard, J., Persson, K., Pietro, J., Prieto, C., Quin, A., van Meter, K., Destouni, G., 2017.
712 Wetlands as large-scale nature-based solutions: Status and challenges for research,
713 engineering and management. *Ecol. Eng.* 108, 489–497.

714 Townend, I., Pethick, J., 2002. Estuarine flooding and managed retreat. *Philos. Trans. A Math.*
715 *Phys. Eng. Sci.* 360 (1796), 1477–1495.

716 van Oyen, T., Carniello, L., D'Alpaos, A., Temmerman, S., Troch, P., Lanzoni, S., 2014. An
717 approximate solution to the flow field on vegetated intertidal platforms: Applicability and
718 limitations. *J. Geophys. Res. Earth Surf.* 119 (8), 1682–1703.

719 van Oyen, T., Lanzoni, S., D'Alpaos, A., Temmerman, S., Troch, P., Carniello, L., 2012. A
720 simplified model for frictionally dominated tidal flows. *Geophys. Res. Lett.* 39 (12), 1–6.

721 Wolters, M., Garbutt, A., Bakker, J.P., 2005. Salt-marsh restoration: Evaluating the success of
722 de-embankments in north-west Europe. *Biol. Cons.* 123 (2), 249–268.